J Therm Anal Calorim (2015) 122:997–1004
DOI 10.1007/s10973-015-4796-5

Effect of polishing waste additive on microstructure and foaming property of porcelain tile and kinetics of sinter-crystallization

Zhiyong Xian[1] · Lingke Zeng[1] · Xiaosu Cheng[1] · Hui Wang[1]

Received: 17 February 2015 / Accepted: 23 May 2015 / Published online: 23 June 2015

Abstract Ceramic tiles were manufactured from an industrial powder batch of porcelain stoneware tiles with 0, 10, 30 and 50 mass% polishing waste and fired at 1100–1180 °C. The phase evolution and microstructure of ceramic tiles with the polishing waste were investigated by X-ray diffraction, differential thermal analysis and scanning electron microscope. The result showed that introduction of the polishing waste into porcelain tiles did not cause significant variations in the phase composition and facilitated the formation of mullite phase. The activation energies of mullite crystallization calculated by the Kissinger method were 780 ± 43, 828 ± 61, 493 ± 18 and 530 ± 30 kJ mol^{-1} for the porcelain tiles with 0, 10, 30 and 50 mass% polishing waste, respectively. In addition, the Avrami constant, *n*, gradually decreased with the increasing polishing waste content, indicating that the crystallization mechanism of mullite in porcelain stoneware tiles changed from two-dimensional crystallization to one-dimensional crystallization. The process of one-dimensional crystallization is more favorable to the formation of needle-shaped mullite and increases the length of mullite.

Keywords Polishing waste · Porcelain tiles · Kinetic crystallization

✉ Xiaosu Cheng
guangzhouscut@163.com

[1] College of Materials Science and Engineering, South China University of Technology, Guangzhou 510640, China

Introduction

Porcelain stoneware tiles are building materials with outstanding technical properties such as mechanical strength, wear and chemical resistance [1–4]. These technical features have made porcelain tiles develop a kind of popular products, whose production grows annually. Porcelain stoneware tiles are usually surface-polished to improve their esthetic aspect and increase the competitiveness with natural stone materials [5, 6]. During the polishing process, the porcelain material in a thickness range of 0.4–0.8 mm from the tile surface is commonly removed, resulting in a large amount of polishing wastes [7–9]. In fact, it has been reported that the output of polishing wastes already exceeds seven million tons per year in China.

Commonly, polishing wastes are collected and temporarily stored in effluent treatment stations, removing the most part of water and producing a mud. Afterward, it is generally disposed in landfill sites. However, the landfill treatment process not only needs to occupy a lot of land, but also leads to waste the mineral resource. In fact, polishing wastes are rich in SiO_2 and Al_2O_3, which are similar to the raw materials used by the building tile industry. Thus, recycling the polishing waste is an attractive way to manufacture traditional building materials. However, the landfill treatment is the main method to deal with the polishing waste in China.

In recent years, some works about utilization of polishing wastes were carried out. Rambaldi et al. [10] studied the recycling of the polishing waste for manufacturing porcelain stoneware tiles, by replacing 10 mass% sodium feldspar sand, which did not cause significant variations in the mechanical strength of the materials. With the polishing waste content increasing, the compact microstructure of the ceramics tile was broken. Shui et al. [11, 12] and

García-Ten et al. [13] reported that polishing wastes used in ceramic bodies prevented the densification process of ceramics due to the existence of SiC. The SiC powder decomposes and forms SiO_2 and CO/CO_2 gas at high temperatures, giving rise to porous microstructures. However, these current studies only focus on the effect of SiC on the microstructure and sintering property of porcelain tiles. They did not really make use of the polishing wastes in the porcelain tiles. In fact, the composition of polishing wastes is complex. The influence of polishing wastes on the phase composition and foaming behaviors of porcelain tiles is still not fully understood. For instance, it is not known how the small amount of mullite derived from polishing wastes affects the crystal phase development and microstructure of the porcelain tile matrix.

In this work, ceramic bodies were prepared from an industrial powder batch of porcelain stoneware tiles with different contents of polishing waste. The phase evolution of ceramic tiles with the polishing waste was investigated by X-ray diffraction, differential thermal analysis and scanning electron microscope. In addition, the effect of polishing waste additive on the process of sinter-crystallization was evaluated.

Experimental

Raw materials

A typical industrial powder batch of porcelain stoneware tiles and a dry polishing waste in form of powder were selected as raw materials. The experimental raw materials were from Newpearl Ceramics Group, Guangdong, China. The compositions of porcelain stoneware tile powders and polishing waste are presented in Table 1. Figure 1 shows the XRD patterns of the porcelain stoneware tile powder and polishing waste. The result indicates that quartz (SiO_2) is the major phase with a small amount of albite ($NaAlSiO_8$), illite ($KMg_3AlSi_3H_2O_{12}$) and kaolinite ($Al_2Si_2H_4O_9$) in the porcelain stoneware tile powder. The polishing waste contains quartz, mullite ($Al_6Si_2O_{13}$), silicon carbide (SiC) and magnesium chloride hydroxide hydrate ($Mg(OH)_2{\cdot}MgCl_2{\cdot}8H_2O$) crystalline phases. The first two are from the polished porcelain tiles, and the others are derived from the polishing tool.

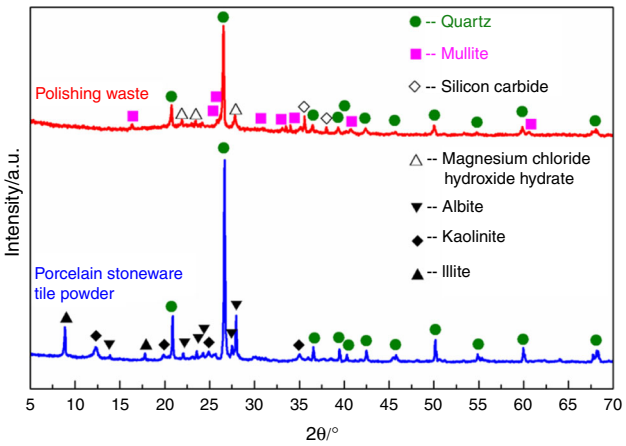

Fig. 1 XRD patterns of porcelain stoneware tile powder and polishing waste

Sample preparation

The studied body mixes were formulated by replacing 0, 10, 30 and 50 mass% of the porcelain stoneware tile powder with the dried polishing waste, respectively. The different studied mixes were prepared by milling in a porcelain jar mill for 30 min, with 35 mass% of water and 0.5 mass% of polyethylene glycol (PEG-400, Guangzhou Taiqi Chemical Technology Co., Ltd., China) as a binder. The raw material powders were subsequently prepared by drying, granulating and sieving with a 30-mesh sieve. The green bodies, in form of disks, were prepared by dry-pressing at 15 MPa. The sintering was performed in a laboratory electric furnace under an air atmosphere at 1100–1180 °C for 10 min at a heating rate of 20 °C min^{-1}.

Characterization

The sintering behaviors such as linear shrinkage, water absorption and bulk density were determined according to the Archimedes method recommended for ceramic tiles, reported in the standard ASTM C373-88 [14]. The crystalline phases of the samples were determined by an X-ray diffractometer (XRD, Philips PW-1710, the Netherlands) using Cu $K\alpha$ radiation. The microstructure morphology of the sintered simples, which were polished and etched by using a 5 % HF solution for 2 min, was observed by scanning electron microscopy (SEM, Philips L30FEG, the

Table 1 Chemical compositions of porcelain stoneware tile powder and polishing waste

Oxides/mass%	SiO_2	Al_2O_3	Fe_2O_3	TiO_2	CaO	MgO	K_2O	Na_2O	IL
Porcelain stoneware tile powder	69.01	22.29	0.44	0.17	0.54	0.48	1.35	4.93	0.6
Polishing waste	67.27	19.21	0.37	0.15	0.62	2.94	1.19	5.17	3.14

IL ignition loss

Netherlands). The thermal analysis of the samples was carried out by a differential thermal analyzer (DTA, STA-449C, Netzsch Instruments Ltd., Germany) from room temperature to 1200 °C at various heating rates (i.e., 5, 10, 15 and 25 °C min^{-1}) under air atmosphere using α-Al_2O_3 as a reference.

Results and discussion

Effect of polishing waste addition on foaming behaviors

Figure 2 shows sintering behaviors of the samples without polishing waste fired at different temperatures. The bulk density initially increases and reaches the maximum value (2.42 g cm^{-3}) at 1160 °C, and then decreases with the increasing temperature. The values of water absorption and open porosity decrease with the increasing temperature and become zero after 1160 °C. These results indicate that the optimum sintering temperature of the porcelain stoneware tile without polishing waste is 1160 °C.

Figure 3 shows sintering behaviors of the samples with different polishing waste contents fired at 1160 °C. The polishing waste content has an influence on the sintering behaviors of the porcelain stoneware tile. When the polishing waste content reaches 30 mass%, the linear shrinkage value falls below zero, which means the fired samples produce volume expansion. In addition, the bulk density gradually decreases with the increasing polishing waste contents. For the sample with 50 mass% polishing waste sintered at 1160 °C, the bulk density is only 0.85 g cm^{-3}.

Microstructure is considered an important parameter regarding the sintering behaviors of fired porcelain body [15]. Figure 4 shows SEM images of the samples with different polishing waste contents fired at 1160 °C. The sample without polishing waste presents a relatively

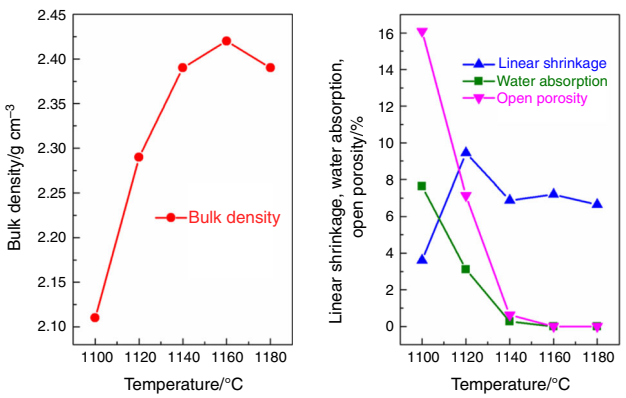

Fig. 2 Sintering behaviors of the samples without polishing waste fired at different temperatures

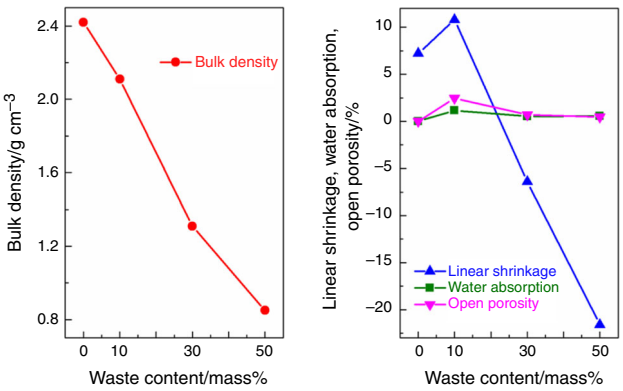

Fig. 3 Sintering behaviors of the samples with different polishing waste contents fired at 1160 °C

compact microstructure with some fine pores (see Fig. 4a). With the polishing waste content increasing, the microstructure of the fired samples becomes weakened. When the polishing waste content is 10 mass%, the sample contains many isolated and spherical pores, and the pore size is about 50 μm, as seen in Fig. 4b. The microstructure of the samples with 30 and 50 mass% polishing waste differs from that of the other samples. A more porous fractured surface can be observed (see Fig. 4c, d), which is attributed to the decomposition of SiC particles from the polishing waste and formation of CO/CO_2 gas. In fact, SiC particles are easy to be oxidized at high temperatures, when they are exposed to oxygen [16, 17]. But the compact SiO_2 protective film formed on the surface of SiC particles can prevent effectively further oxidation of SiC particles. Many previous works [18–20] reported that the flux oxides (i.e., K_2O, Na_2O, CaO and MgO) had a significant corrosive effect on the SiO_2 protective film, which led to a substantial increase in the chemical reaction between SiC and oxygen at relatively low temperatures. Therefore, the fired samples with high content of polishing wastes are more susceptible to foam during sintering due to the abundant flux oxides.

Effect of polishing waste addition on phase evolution

Figure 5 shows XRD patterns of the samples without polishing waste fired at different temperatures. Quartz is the only crystalline phase, and mullite phase cannot be clearly discovered in the samples without polishing wastes. In fact, quartz phase is from residual quartz of raw materials. The low-temperature and fast-firing process is unfavorable to the formation of mullite [21]. In addition, the intensity of the peaks corresponding to quartz gradually decreases with the increasing temperature, which is attributed to the dissolution of quartz in the liquid phase at high firing temperatures. Figure 6 shows XRD patterns of the samples

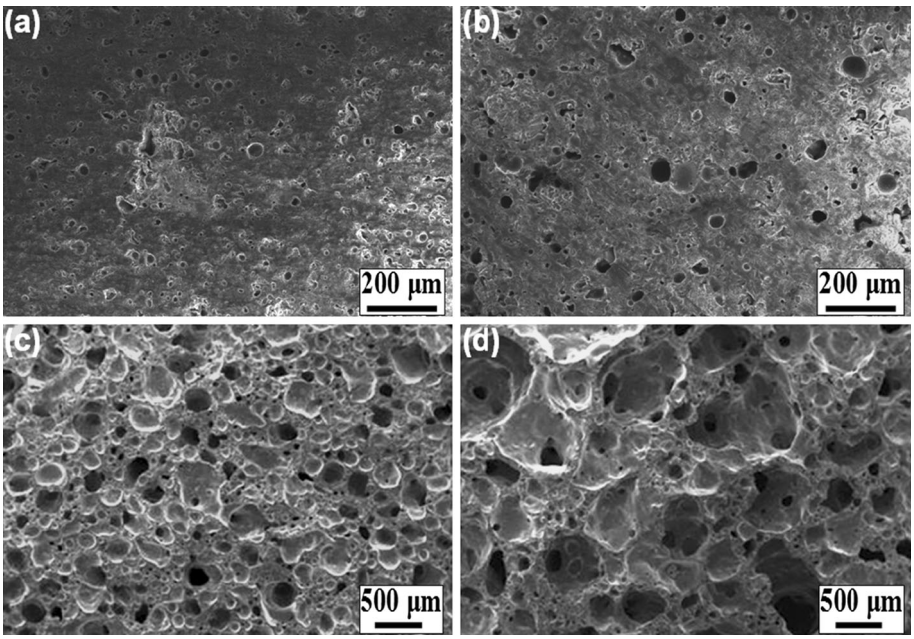

Fig. 4 SEM images of the samples with different polishing waste contents fired at 1160 °C, **a** 0 mass%, **b** 10 mass%, **c** 30 mass% and **d** 50 mass%

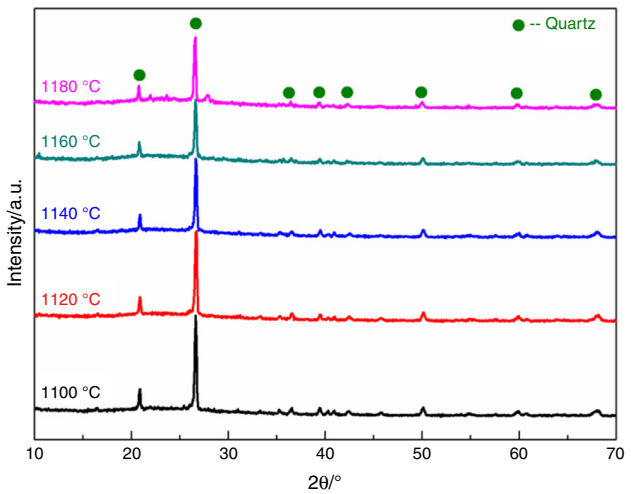

Fig. 5 XRD patterns of the samples without polishing waste fired at different temperatures

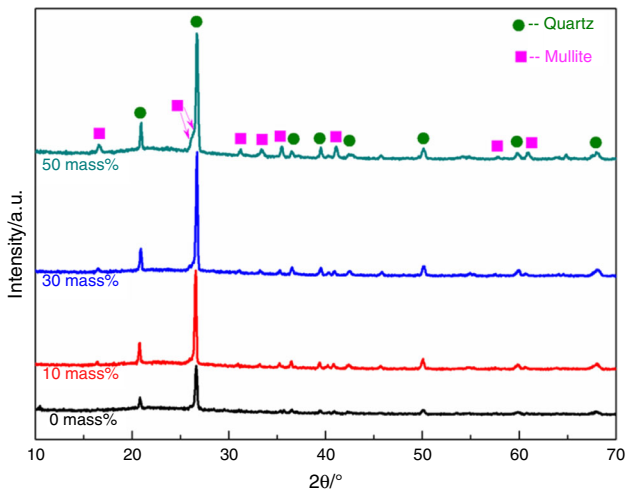

Fig. 6 XRD patterns of the samples with different polishing waste contents fired at 1160 °C

with different polishing waste contents fired at 1160 °C. Quartz and mullite are simultaneously identified in the samples. In addition, the intensity of the peaks corresponding to mullite gradually increases, indicating that mullite content increases with the increasing polishing waste content, which is due to the existence of mullite in the polishing waste (see Fig. 1). Furthermore, the addition of low-temperature flux (i.e., K_2O, Na_2O and MgO) from polishing wastes likewise lowers the temperature of mullite formation [22, 23]. Therefore, introduction of the polishing waste into porcelain stoneware tiles does not cause significant variations in the phase composition and facilitates the formation of mullite phase.

Mechanism and kinetic parameters of sinter-crystallization

Non-isothermal DTA method can be used to analyze the reaction mechanism and calculate the activation energy of crystallization, especially to analyze the kinetics of silicate crystallization [24–26]. Figure 7 shows DTA curves of raw material powders with different polishing waste contents with various heating rates. All the curves exhibit an exothermic peak between 900 and 1100 °C, which is due to the crystallization of mullite. The addition of polishing waste has an impact on the crystallization of mullite, which is effective to reduce the crystallization temperature of mullite.

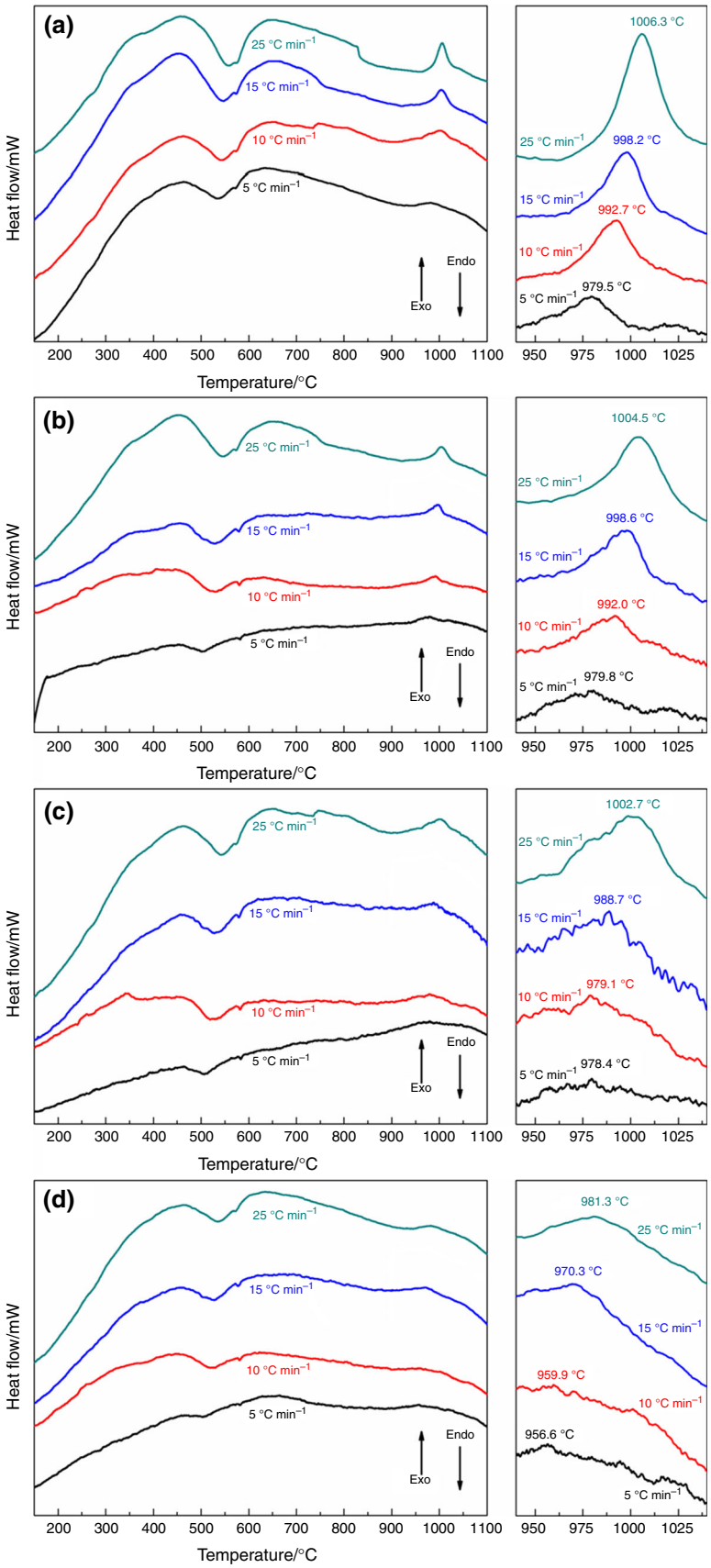

Fig. 7 DTA curves of the raw material powders with different polishing waste contents with heating rate of 5, 10, 15 and 25 °C min^{-1}, **a** 0 mass%, **b** 10 mass%, **c** 30 mass% and **d** 50 mass%

The exothermic peak temperature decreases from 975.5 to 1006.3 °C (the sample without polishing waste) and from 956.6 to 981.3 °C (the sample with 50 mass% polishing waste), which illustrates that the crystallization temperature of mullite decreases about 20 °C. In addition, the intensity of the exothermic peak decreases with the increasing polishing waste content. It confirms that mullite crystallization is related to the transformation of the kaolinite presented in porcelain stoneware formulation [27, 28].

The Kissinger method was proposed to determine the kinetics parameters under non-isothermal conditions [29–31]:

$$\ln\left(\frac{T_m^2}{h}\right) = \frac{E}{RT_m} + \ln\left(\frac{E}{RA}\right) \quad (1)$$

where T_m is the DTA peak temperature, h is the heating rate, and A is the pre-exponential factor. According to Eq. (1), the activation energy can be determined from the slope by plotting $\ln(T_m^2/h)$ versus $1/T_m$, as shown in Fig. 8. It is seen that these plots are linear (coefficient of determination, $r^2 > 0.99$). From the linear slopes, the activation energies of mullite E are determined to be 780 ± 43, 828 ± 61, 493 ± 18 and 530 ± 30 kJ mol^{-1} for the samples with 0, 10, 30 and 50 mass% polishing waste, respectively. It is indicated that the addition of polishing waste into porcelain stoneware tiles makes the activation energy of mullite crystallization decrease, which is due to the existence of mullite in the polishing waste. Mullite as a seed can promote the crystallization of mullite. Vilmin et al. [32] found that zircon seeds could lower the zircon crystallization temperature. Zhang et al. [33] also reported that the introduction of seeds into the leucite precursor could significantly lower the leucite crystallization temperature. The crystal growth process can occur more readily in the case of a smaller activation energy with a lower crystallization energy barrier [24].

In fact, the value of E reflects the temperature sensitivity of the crystallization process. The activation energies for nucleation growth of mullitization from monophasic gels, diphasic gels, hybrid gels, glass fibers and kaolinites have been examined by many workers using isothermal and/or non-isothermal methods [34–38]. The reported E values from monophasic gels and kaolinites are about 300–530 kJ mol^{-1} [34, 38], while those from diphasic gels, hybrid gels and glass fibers are about 800–1300 kJ mol^{-1} [35–37], more than twice as large as for the former group. The differences in these E values may be due to the differences in the crystallization processes mentioned above or due to experimental conditions and sample impurities. Based on this point, it is reasonable to infer that the crystallization kinetics of mullite crystallization in porcelain stoneware tiles will also change with the addition of polishing wastes.

Using the activation energies calculated, we can determine the Avrami constant, n, corresponding to the crystallization mechanism [39] as:

$$n = \frac{2.5}{\Delta T} \cdot \frac{RT_m^2}{E} \quad (2)$$

where ΔT is the full width at half maximum of the exothermic peak. The value of ΔT can be calculated by the *curve fit* function of Origin 8.0 software [40]. The value of the Avrami constant provides the information regarding the morphology of the growing crystals [25]. The value of n close to one means that one-dimensional growth dominates the overall crystallization, the value of two indicates the two-dimensional crystallization, the value of three implies a significant contribution of three-dimensional growth, and the value of four indicates the homogeneous crystallization [41–43].

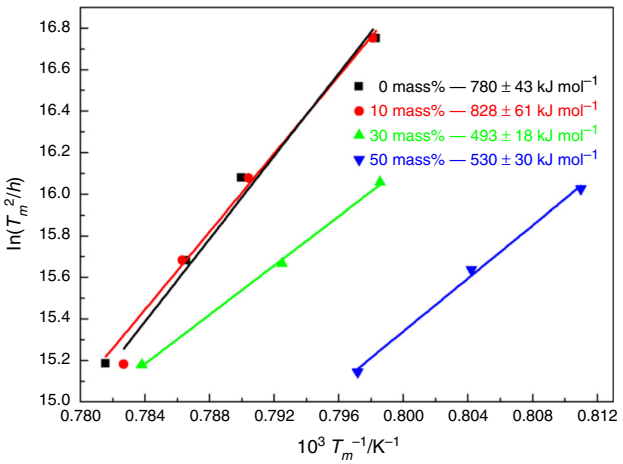

Fig. 8 Plots of $\ln(T_m^2/h)$ versus $10^3/T_m$ for the raw material powders with different polishing waste contents

Table 2 Calculated values of the Avrami constant, n

Polishing waste content/mass%	h/°C min^{-1}	n	$n_{average}$
0	5	1.44	1.82
	10	1.88	
	15	2.16	
	25	1.80	
10	5	1.09	1.59
	10	1.69	
	15	1.85	
	25	1.73	
30	10	1.41	1.50
	15	1.57	
	25	1.53	
50	10	1.07	1.12
	15	1.15	
	25	1.16	

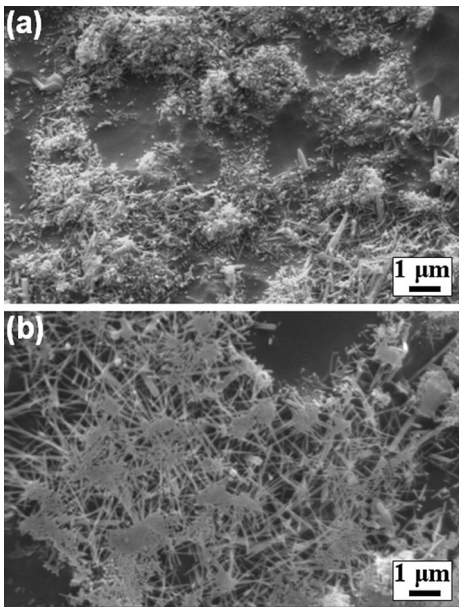

Fig. 9 SEM images of samples with different polishing waste contents fired at 1160 °C, **a** 0 mass% and **b** 50 mass%

Table 2 shows the calculated values of the Avrami constant of the samples with different polishing waste contents. The value of n gradually decreases, and the samples crystallization mechanism changes from two-dimensional crystallization to one-dimensional crystallization with the polishing waste addition.

Figure 9 shows the SEM images of the fired samples without and with 50 mass% polishing waste. A large amount of mullite wrapped in the glassy matrix is detected. In addition, for the sample with 50 mass% polishing waste, the length of mullite is much longer than that of the sample without polishing waste. The SEM result is consistent with that of the calculated n value. The process of one-dimensional crystallization is more favorable to the formation of needle-shaped mullite. In addition, one of the oldest theories on the strength of porcelain, the mullite hypothesis [44, 45], suggests that porcelain strength depends on the interlocking of fine mullite needles. Furthermore, fibrous mullite distributed in the glass matrix grows a three-dimensional network, which can lead to significantly increased resistance to pyroplastic deformation [46].

Conclusions

In the present study, ceramic tiles were prepared by adding different polishing waste contents into an industrial powder batch and fired at different temperatures. The influence of the content of polishing waste on foaming behavior, phase evolution and kinetics crystallization of porcelain tiles was investigated. The crystallization temperature of mullite in porcelain stoneware tiles decreased with the increasing polishing waste contents. The activation energies of mullite crystallization calculated by the Kissinger method were 780 ± 43, 828 ± 61, 493 ± 18 and 530 ± 30 kJ mol^{-1} for the samples with 0, 10, 30 and 50 mass% polishing waste, respectively.

The Avrami constant, n, gradually decreased with the increasing polishing waste content, indicating that the crystallization mechanism of mullite in porcelain stoneware tiles changed from two-dimensional crystallization to one-dimensional crystallization. The process of one-dimensional crystallization is more favorable to the formation of needle-shaped mullite.

Acknowledgements This work was supported by the ChanXueYan Special Funds of Guangdong (No. 2012B091100306).

References

1. Sanchez E, Garcia-Ten J, Sanz V, Moreno A. Porcelain tile: almost 30 years of steady scientific-technological evolution. Ceram Int. 2010;36:831–45.
2. Jorge MM, Jesus MR, Maximina R. Effect of microstructure on mechanical properties of porcelain stoneware. J Eur Ceram Soc. 2010;30:3063–9.
3. Santos GRdos, Salvetti AR, Cabrelon MD, Morelli MR. Synthetic flux as a whitening agent for ceramic tiles. J Therm Anal Calorim. 2014;615:S459–61.
4. Acchar W, Dultra EJV. Thermal analysis and X-ray diffraction of untreated coffee's husk ash reject and its potential use in ceramics. J Therm Anal Calorim. 2013;111:1331–4.
5. Sanchez E, Ibanez MJ, Garcia-Ten J, Quereda MF, Hutchings IM, Xu YM. Porcelain tile microstructure: implications for polished tile properties. J Eur Ceram Soc. 2006;26:2533–40.
6. Dondi M, Ercolani G, Guarini G, Melandri C, Raimondo M, Almendra E, Cavalcante P. The role of surface microstructure on the resistance to stains of porcelain stoneware tiles. J Eur Ceram Soc. 2005;25:357–65.
7. Alves HJ, Freitas MR, Melchiades FG, Boschi AO. Dependence of surface porosity on the polishing depth of porcelain stoneware tiles. J Eur Ceram Soc. 2011;31:665–71.
8. Gabaldón-Estevan D, Criado E, Monfort E. The green factor in European manufacturing: a case study of the Spanish ceramic tile industry. J Clean Prod. 2014;70:242–50.
9. Silva J, de Brito J, Veiga R. Recycled red-clay ceramic construction and demolition waste for Mortars production. J Mater Civ Eng. 2010;22:236–44.
10. Rambaldi E, Esposito L, Tucci A, Timellini G. Recycling of polishing porcelain stoneware residues in ceramic tiles. J Eur Ceram Soc. 2007;27:3509–15.
11. Shui AZ, Xi XA, Wang YM, Cheng XS. Effect of silicon carbide additive on microstructure and properties of porcelain ceramics. Ceram Int. 2011;37:1557–62.
12. Xi XA, Xu LF, Shui AZ, Wang YM, Naito M. Effect of silicon carbide particle size and CaO content on foaming properties during firing and microstructure of porcelain ceramics. Ceram Int. 2014;40:12931–8.

13. García-Ten J, Saburit A, Bernardo E, Colombo P. Development of lightweight porcelain stoneware tiles using foaming agents. J Eur Ceram Soc. 2012;32:745–52.
14. Christogerou A, Kavas T, Pontikes Y, Koyas S, Tabak Y, Angelopoulos GN. Use of boron wastes in the production of heavy clay ceramics. Ceram Int. 2009;35:447–52.
15. Cheng XS, Ke SJ, Wang QH, Wang H, Shui AZ, Liu PA. Fabrication and characterization of anorthite-based ceramic using mineral raw materials. Ceram Int. 2012;38:3227–35.
16. Xi XA, Shui AZ, Li YF, Wang YM, Abe H, Naito M. Effects of magnesium oxychloride and silicon carbide additives on the foaming property during firing for porcelain ceramics and their microstructure. J Eur Ceram Soc. 2012;32:3035–41.
17. Radtke C, Brandao RV, Pezzi RP, Morais J, Baumvol IJR, Stedile FC. Characterization of SiC thermal oxidation. Nucl Instrum Methds Phys Res B. 2002;190:579–82.
18. Jacobson NS. Kinetics and mechanism of corrosion of SiC by molten salts. J Am Ceram Soc. 1986;69:74–82.
19. Fox DX, Smialek JL. Burner rig hot corrosion of silicon carbide and silicon nitride. J Am Ceram Soc. 1990;73:303–11.
20. Feber MK, Ogle J, Tennery VJ, Henson V. Characterization of corrosion mechanisms in a sintered SiC exposed to basic coal slags. J Am Ceram Soc. 1985;68:191–7.
21. Martín-Márquez J, Rincón JM, Romero M. Mullite development on firing in porcelain stoneware bodies. J Eur Ceram Soc. 2010;30:1599–607.
22. Hojamberdiev M, Eminov A, Xu YH. Utilization of muscovite granite waste in the manufacture of ceramic tiles. Ceram Int. 2011;37:871–6.
23. Belhouchet H, Hamidouche M, Torrecillas R, Fantozzi G. The non-isothermal kinetics of mullite formation in boehmite-zircon mixtures. J Therm Anal Calorim. 2014;116:795–803.
24. Tkalcec E, Kurajica S, Ivankovic H. Diphasic aluminosilicate gels with two stage mullitization in temperature range of 1200–1300 °C. J Eur Ceram Soc. 2005;25:613–26.
25. Johnson BR, Kriven WM, Schneider J. Crystal structure development during devitrification of quenched mullite. J Eur Ceram Soc. 2001;21:2541–62.
26. Takei T, Kameshima Y, Yasumori A. Crystallization kinetics of mullite from Al_2O_3–SiO_2 glasses under non-isothermal conditions. J Eur Ceram Soc. 2001;21:2487–93.
27. Djangang CN, Tchamba AB, Kamseu E, Melo UC, Elimbi A, Ferrari AM, Leonelli C. Reaction sintering and microstructural evolution in metakaolin-metastable alumina composites. J Therm Anal Calorim. 2014;117:1035–45.
28. Kaljuvee T, Stubna I, Somelar P, Mikli V, Kuusik R. Thermal behavior of some Estonian clays and their mixtures with oil shale ash additives. J Therm Anal Calorim. 2014;118:891–9.
29. Kissinger HE. Variations of peak temperature with heating rate in differential thermal analysis. J Res Nat1 Bur Stnd. 1956;57: 217–21.
30. El-Karsani KSM, Al-Muntasheri GA, Sultan AS, Hussein IA. Gelation kinetics of PAM/PEI system DSC investigation. J Therm Anal Calorim. 2014;116:1409–15.
31. Fandaruff C, Araya-Sibaja AM, Pereira RN, Hoffmeister CRD, Rocha HVA, Silva MAS. Thermal behavior and decomposition kinetics of efavirenz under isothermal and non-isothermal conditions. J Therm Anal Calorim. 2014;115:2351–6.
32. Vilmin G, Komarneni S, Roy R. Lowering crystallization temperature of zircon by nanoheterogeneous sol–gel processing. J Mater Sci. 1987;22:3556–60.
33. Zhang Y, Li B, Rao PG, Lv M, Wu JQ. Seeded crystallization of leucite. J Am Ceram Soc. 2007;90:1615–8.
34. Li DX, Thomson WJ. Mullite formation kinetics of a single-phase gel. J Am Ceram Soc. 1990;73:964–9.
35. Lee JS, Yu SC. Mullite formation kinetics of coprecipitated Al_2O_3-SiO_2 gels. Mater Res Bull. 1992;27:405–16.
36. Huling JC, Messing GL. Epitactic nucleation of spinel in aluminosilicate gels and its effect on mullite crystallization. J Am Ceram Soc. 1991;74:2374–81.
37. Takei T, Kameshima Y, Yasumori A, Okada K. Crystallization kinetics of mullite in alumina-silica glass fibers. J Am Ceram Soc. 1999;82:2876–80.
38. Gualtieri A, Bellotto M, Artioli G, Clark SM. Kinetic study of the kaolinite-mullite reaction sequence. Part II: mullite formation. Phys Chem Miner. 1995;22:215–22.
39. Augis JA, Bennet JE. Calculation of the avrami parameters for heterogeneous solid state reactions using a modification of the Kissinger method. J Therm Anal Calorim. 1978;13:283–92.
40. Ke SJ, Wang YM, Pan ZD. Crystallization kinetics of neodymium disilicate obtained by polymeric xerogels. J Mater Sci. 2014;49:3736–41.
41. Clupper DC, Hench LL. Crystallization kinetics of tape cast bioactive glass 45S5. J Non Cryst Solids. 2003;318:43–8.
42. EI-Shennawi AWA, Hamzawy EMA, Khater GA, Omar AA. Crystallization of some aluminosilicate glasses. Ceram Inter. 2001;27:725–30.
43. Romero M, Rincon JM, Acosta A. Effect of iron oxide content on the crystallisation of a diopside glass-ceramic glaze. J Eur Ceram Soc. 2002;22:883–90.
44. Stathis G, Ekonomakou A, Stournaras CJ, Ftikos C. Effect of firing conditions, filler grain size and quartz content on bending strength and properties of sanitaryware porcelain. J Eur Ceram Soc. 2004;24:2357–66.
45. Capoglu A. A novel low-clay translucent whiteware based on anorthite. J Eur Ceram Soc. 2011;31:321–9.
46. Senapati U, Carty WM. Porcelain-raw materials, processing, phase evolution, and mechanical behavior. J Am Ceram Soc. 1998;81:3–20.